Effect of proton irradiation on superconductivity in optimally doped $BaFe_2(As_{1-x}P_x)_2$ single crystals

M. P. Smylie,[1,*] M. Leroux,[1] V. Mishra,[1,†] L. Fang,[1] K. M. Taddei,[1,2] O. Chmaissem,[1,2] H. Claus,[1] A. Kayani,[3] A. Snezhko,[1] U. Welp,[1] and W.-K. Kwok[1]

[1]*Materials Science Division, Argonne National Laboratory, 9700 South Cass Avenue, Argonne, Illinois 60439, USA*

[2]*Department of Physics, University of Northern Illinois, DeKalb, Illinois 60115, USA*

[3]*Department of Physics, Western Michigan University, Kalamazoo, Michigan 49008, USA*

(Received 24 July 2015; published 10 March 2016)

Irradiation with 4 MeV protons was used to systematically introduce defects in single crystals of the iron-arsenide superconductor $BaFe_2(As_{1-x}P_x)_2$, $x = 0.33$. The effect of disorder on the low-temperature behavior of the London penetration depth $\lambda(T)$ and transition temperature T_c was investigated. In nearly optimally doped samples with $T_c \sim 29$ K, signatures of a superconducting gap with nodes were observed. Contrary to previous reports on electron-irradiated crystals, we do not see a disorder-driven lifting of accidental nodes, and we observe that proton-induced defects are weaker pair breakers than electron-induced defects. We attribute our findings to anisotropic electron scattering caused by proton irradiation defects.

DOI: 10.1103/PhysRevB.93.115119

Introduction. The structure of the superconducting gap and pairing mechanism of iron-based superconductors has been the subject of extensive research. Due to the magnetic nature of the parent compounds of many different families of iron-based superconductors, a spin fluctuation mediated pairing mechanism has been proposed in theoretical studies, which is also supported by various experimental results [1–6]. Spin fluctuation mediated pairing is thought to give rise to the $s_\pm$ state with a relative phase of π in the superconducting order parameters on the electron and hole bands [2,3,7]. In some cases, accidental nodes in the order parameter may appear on some Fermi surface sheets. Experimentally identifying the structure of the order parameter is a major challenge, due to the complicated multiband electronic structure.

The effect of impurities on superconductors is very sensitive to the nature of the gap [8,9]. For conventional s-wave superconductors, ordinary nonmagnetic impurities do not affect superconductivity [10,11]. On the other hand, nonmagnetic impurities act as strong pair breakers in a superconductor with nodes. In addition, in a multiband superconductor the effects of inter- and intraband scattering need to be considered. For $s_\pm$ symmetry, nonmagnetic interband scattering is pair breaking and will reduce T_c, whereas nonmagnetic intraband scattering only affects T_c in the presence of nodes. However, in this work nonmagnetic intraband scattering is dominant in suppressing T_c. Furthermore, the temperature dependence of the low-temperature penetration depth $\lambda(T)$ can be used to distinguish between nodal and fully gapped superconductors [12–14]. In an isotropic s-wave superconductor, the penetration depth has an exponential temperature dependence due to the energy gap in the excitation spectrum, whereas for d-wave superconductors with line nodes λ varies linearly with the temperature [15]. In multiband superconductors, the temperature dependence of the penetration depth at low temperatures ($T \leqslant T_c/3$) is dominated by the bands with nodes or with a nonzero density of states at the Fermi energy. However, interband impurity scattering is pair breaking and induces midgap impurity states [16] which gives rise to a power-law temperature dependence of the penetration depth with a power close to 2 in the dirtier systems. As a result, the temperature dependence of the low-temperature penetration depth changes from linear to quadratic with increasing pair-breaking scattering [15,17,18]. In superconductors with accidental nodes, addition of disorder is expected to lift, or wash out, the nodes and to create a small gap in the excitation spectrum, which modifies the low-T penetration depth [19]. This is true even if the nodes have complicated three-dimensional structure [20]; for $BaFe_2As_2$-derived superconductors there are theoretical proposals [21–24] for and experimental indications of a three-dimensional nature of the nodal structure of the gap function. However, such three-dimensional structure is not expected to change the temperature dependence of the penetration depth qualitatively [20]. Wang *et al.* have shown that in superconductors with accidental nodes, the nodes may reappear in the presence of interband scattering [25]. This leads from linear to exponential behavior followed by a quadratic temperature dependence in the penetration depth with increasing disorder. Such behavior has been recently observed experimentally by Mizukami *et al.* in $BaFe_2(As_{1-x}P_x)_2$ irradiated with 2.5 MeV electrons [26].

Systematic defect creation using particle irradiation has been exploited as a tool to study the gap structure in many different superconductors. Depending on the type of irradiating particles and energy of the beam, one can form isolated point defects, clusters of point defects, extended defects such as columnar or disklike defects, or combinations of various types. Electron irradiation is a very efficient method to create isolated point defects. Irradiation with heavy ions can lead to the formation of columnar defects, which are very important from the point of vortex pinning enhancement [27,28]. Proton irradiation creates cascades of point defects along with isolated point defects [29–31].

In this paper, we report on the effect of disorder induced with 4 MeV proton irradiation on nearly optimally doped $BaFe_2(As_{1-x}P_x)_2$ single crystals. Our penetration depth measurements confirm the presence of gap nodes near optimal doping. However, we do not see the node-lifting phenomenon

*Corresponding author: msmylie@anl.gov

†Present address: Center for Nanophase Materials Sciences, Oak Ridge National Laboratory, Oak Ridge, Tennessee 37831, USA.

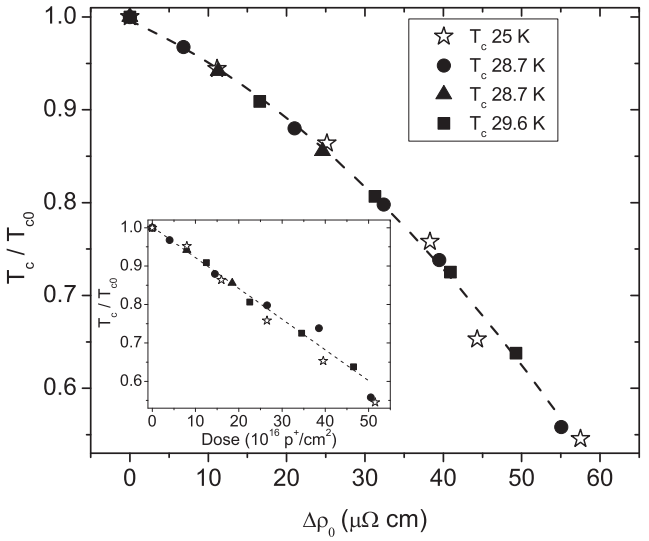

FIG. 1. Suppression of transition temperature T_c as a function of increase in extrapolated zero-temperature resistivity in $BaFe_2(As_{1-x}P_x)_2$ single crystals. The legend indicates the initial T_c of each crystal before irradiation. The line is a guide to the eye. The inset shows the normalized T_c from dc SQUID magnetization (filled shapes) and transport measurements (stars) as a function of irradiation dose.

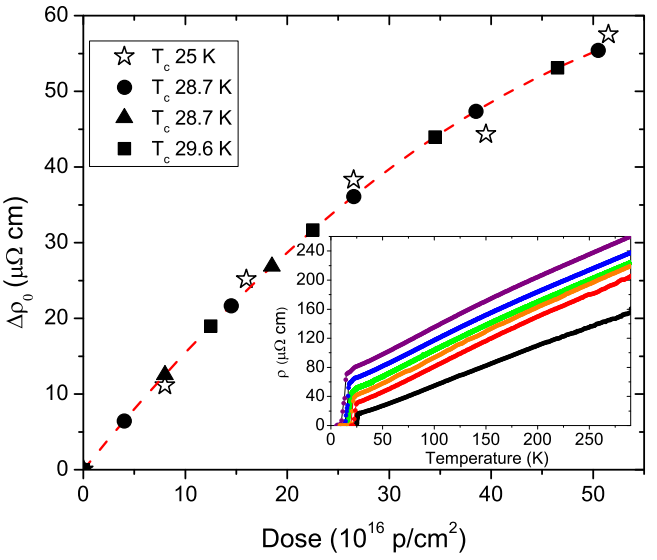

FIG. 2. Increase in extrapolated zero-temperature resistivity as a function of irradiation dose for SQUID samples (solid shapes) and transport sample (stars). The line is a guide to the eye. The inset shows the resistivity of a $BaFe_2(As_{1-x}P_x)_2$ crystal with $T_{c0} \sim 25$ K as a function of temperature for various irradiation doses; as the dose increases, the normal-state resistivity increases.

observed with electron irradiation in Ref. [26] in a similar temperature range. Our study suggests that defects induced by protons are weaker pair breakers than those created by electrons and that anisotropy strongly modifies the effect of impurity scattering on the superconducting gap.

Experimental details. Single crystals of high-purity $BaFe_2(As_{1-x}P_x)_2$ were grown using a self-flux method, and crystals were cut into 300×400 μm^2 rectangles approximately 20 μm thick. Three crystals with nearly optimal doping ($x = 0.33$) were chosen for examination, two with $T_c \sim 28.7$ K and one with $T_c \sim 29.6$ K. Additionally, a larger bar (550 μm$\times$ 930 μm $\times$ 70 μm) from a different batch with $T_c \sim 25$ K and a room-temperature resistivity of 120 $\mu\Omega$ cm was selected for transport measurements. This resistivity value is comparable to reported results [32,33]. All samples were repeatedly irradiated at the tandem Van de Graaff accelerator at Western Michigan University with 4 MeV protons, with characterization performed in between successive irradiation runs. A gold foil was used to disperse the beam to ensure a uniform beam spot over the samples, and the irradiation stage was cooled to $\sim -10^\circ$ C during irradiation. TRIM calculations for our irradiation geometry show that proton implantation is negligible [34].

Results and discussion. For the three samples, we determined the transition temperature (T_c) from the magnetization data, acquired on a custom SQUID magnetometer; the value of T_c is taken at the half-height of the transition; see the inset of Fig. 3(a). We find a strong suppression of T_c with increasing irradiation dose. The variation of T_c, normalized to the respective transition temperature of the pristine sample (T_{c0}), as a function of irradiation dose is shown in the inset of Fig. 1. The transition temperature is suppressed linearly with increasing dose, even at a fairly high dose of 50×10^{16} p/cm^2. The fact that all of the samples follow this trend indicates that the effect of irradiation-induced defects on electron scattering and pair breaking is the same in all of the samples even though the initial T_c values are slightly different. The initial transition width observed on all three crystals is sharp, indicating high-quality single-phase material. The transitions remain sharp with increasing total proton dose, demonstrating that the crystal remains single phase over the entire range of irradiation. Furthermore, the change in T_c never saturates with increasing dose, showing that the system remains dominated by interband scattering.

Resistivity measurements were performed in a continuous flow liquid helium cryostat with a standard 4-point contact technique. The temperature dependence of the resistivity is plotted for several irradiation levels in the inset of Fig. 2. Following the initial irradiation dose, subsequent irradiations do not change the curvature of ρ vs T, but only offset the curves, consistent with an increase in ρ_0. Figure 2 shows the change in the extrapolated zero-temperature resistivity with irradiation dose. This quantity is directly related to the scattering processes caused by the irradiation-induced defects. We observe nearly linear behavior for small doses, indicating a linear increase in the number of defects for lower doses, followed by a sublinear growth and tendency towards saturation at higher doses [35].

For the transport sample, the reduced T_c versus increase in ρ_0 was directly taken from the transport measurements. The effective increase in ρ_0 for the SQUID samples had to be inferred by fitting a parabolic function to the ρ_0 data, Fig. 2. By plotting the SQUID sample dose levels on this curve, the effective increase in ρ_0 for all dose levels could be estimated, resulting in the data shown in Fig. 1.

The initial decrease in T_c with respect to increasing $\Delta\rho_0$ is approximately 0.15 K/$\mu\Omega$ cm. This T_c suppression

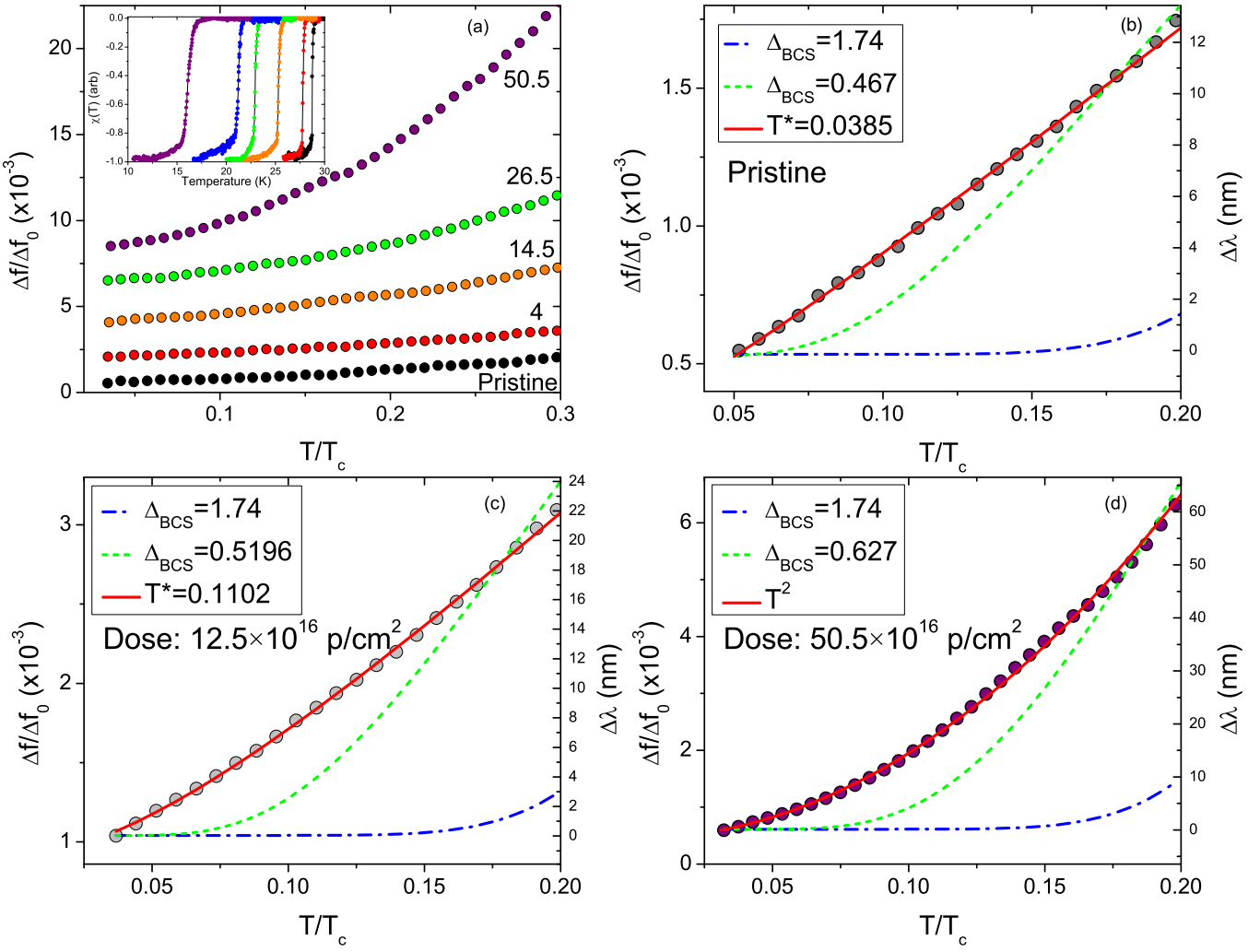

FIG. 3. Effect of increasing irradiation dose on the change in the resonator frequency (Δf) measured on a $BaFe_2(As_{1-x}P_x)_2$ single crystal with $T_{c0} \sim 29$ K. Panel (a) displays the evolution of Δf with increasing proton dose indicated in units of 10^{16} p/cm^2; the curves are offset by 0.002 along the y axis for clarity. The inset shows T_c decreasing with dose and how transitions remain sharp as dose increases in SQUID magnetization data. Panels (b), (c), and (d) show Δf data at zero, intermediate, and high dose, respectively, together with various fits. Data in (b) and (c) are well described by the HG function (red lines) whereas the high-dose data follow a T^2 dependence. At no dose is it possible to fit the data with a BCS-like exponential dependence with a fixed (blue lines) or free (green) gap parameter. The same trends were observed in three crystals, and the data shown are characteristic of the whole set.

is weaker as compared to the rate of $\sim$0.3 K/$\mu\Omega$ cm obtained with electron irradiation [26]. A survey of published data reveals that the T_c suppression due to electron irradiation is in general larger than with proton irradiation. In isovalently doped $Ba(Fe_{1-x}Ru_x)_2As_2$ electron irradiation induced T_c suppression at the rate [36] of $\sim$0.35 K/$\mu\Omega$ cm whereas for optimally doped $Ba_{1-x}K_xFe_2As_2$ the rate [37] is $\sim$0.2 K/$\mu\Omega$ cm; the rate of suppression is higher in underdoped samples. In contrast, proton irradiation of optimally doped $Ba(Fe_{1-x}Co_x)_2As_2$ [35,38] and $Ba_{1-x}K_xFe_2As_2$ [39] yielded T_c suppression of 0.16 K/$\mu\Omega$ cm and 0.1 K/$\mu\Omega$ cm, respectively. The rate of suppression is a direct measure of pair-breaking scattering, and low values of the strength of the suppression rate suggest that the defects generated by proton irradiation act as weaker pair breakers than the defects coming from electron irradiation.

The low-temperature variation of the penetration depth $\Delta\lambda(T)$ provides direct information about the low-energy quasiparticle excitation spectrum. For three crystals, the magnetic penetration depth was measured with a custom tunnel diode oscillator (TDO) system operating at $\sim$14.5 MHz down to 500 mK. In this technique, the frequency shift Δf of the resonator is proportional to the change of the penetration depth, $\Delta f = G\Delta\lambda$, where the geometrical factor G depends on the sample volume and shape, and also the geometry of the resonator coil; G was determined for each sample using a standard procedure [40]. Figure 3(a) summarizes the evolution of the low-temperature TDO response of $BaFe_2(As_{1-x}P_x)_2$ crystals at various stages of proton irradiation. We illustrate in Fig. 3 the low-temperature power-law behavior of the penetration depth that is an indicator of gap nodes. This agrees with earlier work by Hashimoto *et al.* showing the presence of line nodes from thermal transport and penetration depth measurements [41,42], and NMR studies by Nakai *et al.* [43]. The temperature variations of the frequency shift at various irradiation stages can be fitted to the

TABLE I. T_c suppression and low-temperature fitting parameter T^* of the penetration depth as a function of proton dose.

Dose (10^{16} p/cm^2)	T_c/T_{c0}	T^* (K)
0	1	0.0385
4	0.966	0.09
12.5	0.909	0.1102
14.5	0.879	0.382
22.5	0.807	T^2
26.5	0.797	T^2
34.5	0.725	T^2
38.5	0.739	T^2
46.5	0.638	T^2
50.5	0.572	T^2

Hirschfeld-Goldenfeld (HG) form [15], originally proposed for a d-wave superconductor with line nodes, $\Delta\lambda = AT^2/(T + T^*)$, where T^* is a measure of disorder in the system and A is a fitting parameter which accounts for all the geometrical factors. For pristine samples, the penetration depth varies essentially linearly with temperature as shown in Fig. 3(b). The samples do show small intrinsic disorder, as evidenced by the finite, small value of $T^* = 0.04$ K in the HG function. With increasing doses of irradiation, the value of T^* grows; see Figs. 3(c) and 3(d) and Table I. The penetration depth can still be fitted with the HG function up until a critical dose, above which the penetration depth can only be fitted as T^2. We also note that the absence of an upturn in Δf at low temperatures shows that p-irradiation-induced defects are nonmagnetic [26,44,45].

In contrast to recent reports by Mizukami *et al.*, at no dose level in any of our crystals do we observe the emergence of a full gap in our proton-irradiated samples even though we cover the same range of T_c suppression and the same measured temperature range as in Ref. [26]. A possible explanation lies in the different structure of electron and proton irradiation induced defects. Irradiation with MeV electrons produces predominantly low-energy recoils resulting in the formation of pairs of point defects (Frenkel pairs), whereas MeV-proton irradiation yields recoils with energies up to keV resulting in a mixture of point defects and small collision cascades [29]. Extensive transmission electron microscopy (TEM) work on proton-irradiated $YBa_2Cu_3O_7$ revealed anisotropic collision cascades of roughly 2–4 nm in size [46,47]. At present, no such studies exist for $BaFe_2(As_{1-x}P_x)_2$. Although the details of the irradiation-induced defect structure will depend on the material at hand and on the preexisting defects, numerical simulations [48] using TRIM software [34] indicate that proton irradiation of $BaFe_2(As_{1-x}P_x)_2$ produces a mixture of point defects and nm-sized, possibly anisotropic, cascades. The scattering potential due to point defects is composed of essentially isotropic contributions from Fourier components with wave vectors spanning the entire range, including large wave vectors that span the Brillouin zone. These effectively mix the electron states on the hole and electron Fermi surface sheets causing suppression of T_c. In contrast, the cascades, owing to their extended size, are most likely to yield anisotropic scattering at selected wave vectors [49] and small-angle scattering, that is, intraband scattering. Both intraband and interband scattering contribute to the electrical resistance; however, interband scattering is dominant in pair breaking in an $s_\pm$ superconductor. Thus, it is expected that the rate of suppression of T_c (with respect to increase in residual resistivity) due to proton irradiation is lower as not all defects contribute to interband pair breaking. Furthermore, since the isotropic mixing of states (as assumed in Refs. [19,20,25]) does not arise in the case of the extended cascades, it is conceivable that the node lifting is not complete in this case or that a complete gap is significantly smaller than in the corresponding case of electron irradiation such that it cannot be detected in our current temperature range.

In summary, we present measurements of the magnetization, resistivity, and magnetic penetration depth of pristine and proton-irradiated $BaFe_2(As_{1-x}P_x)_2$ crystals. Upon proton irradiation, T_c is continuously suppressed with the transitions staying sharp, and the residual resistivity is increased. The low-temperature variation of the penetration depth of the pristine samples is linear, indicative of line nodes in the superconducting gap. The evolution of the temperature dependence of the penetration depth with irradiation is well described by the Hirschfeld-Goldenfeld relation for moderate irradiation doses. At high doses, the temperature dependence is simply quadratic as expected for a disordered superconductor with line nodes. At no dose level in our proton-irradiated samples and for none of our crystals do we observe the emergence of a full gap as has been reported [26] for a narrow range of T_c suppression of electron-irradiated $BaFe_2(As_{1-x}P_x)_2$ crystals. We attribute this to the difference in electron scattering due to pointlike electron-irradiation-induced defects and extended collision cascades due to proton irradiation.

Acknowledgments. Tunnel diode oscillator and magnetization measurements were supported by the US Department of Energy, Office of Science, Basic Energy Sciences, Materials Sciences and Engineering Division. Theoretical work and transport measurements (V.M., M.L.) and synthesis (L.F., K.T.) were supported by the Center for Emergent Superconductivity, an Energy Frontier Research Center funded by the US DOE, Office of Science, Office of Basic Energy Sciences.

[1] D. C. Johnston, Adv. Phys. **59**, 803 (2010).
[2] P. C. Canfield and S. L. Bud'ko, Annu. Rev. Condens. Matter Phys. **1**, 27 (2010).
[3] P. J. Hirschfeld, M. M. Korshunov, and I. I. Mazin, Rep. Prog. Phys. **74**, 124508 (2011).
[4] G. R. Stewart, Rev. Mod. Phys. **83**, 1589 (2011).
[5] H. H. Wen and S. Li, Annu. Rev. Condens. Matter Phys. **2**, 121 (2011).
[6] A. V. Chubukov, Annu. Rev. Condens. Matter Phys. **3**, 57 (2012).
[7] I. I. Mazin, D. J. Singh, M. D. Johannes, and M. H. Du, Phys. Rev. Lett. **101**, 057003 (2008).

[8] A. V. Balatsky, I. Vekther, and J.-X. Zhu, Rev. Mod. Phys. **78**, 373 (2006).

[9] H. Alloul, J. Bobroff, M. Gabay, and P. J. Hirschfeld, Rev. Mod. Phys. **81**, 45 (2009).

[10] P. W. Anderson, J. Phys. Chem. Solids **11**, 26 (1959).

[11] A. A. Abrikosov and L. P. Gor'kov, Zh. Eksp. Teor. Fiz. **39**, 1781 (1960) [Sov. Phys. JETP **12**, 1243 (1961)].

[12] R. Prozorov, R. W. Giannetta, P. Fournier, and R. L. Greene, Phys. Rev. Lett. **85**, 3700 (2000).

[13] A. Snezhko, R. Prozorov, D. D. Lawrie, R. W. Giannetta, J. Gauthier, J. Renaud, and P. Fournier, Phys. Rev. Lett. **92**, 157005 (2004).

[14] R. Prozorov and R. W. Giannetta, Supercond. Sci. Technol. **19**, R41 (2006).

[15] P. J. Hirschfeld and N. Goldenfeld, Phys. Rev. B **48**, 4219 (1993).

[16] A. B. Vorontsov, M. G. Vavilov, and A. V. Chubukov, Phys. Rev. B **79**, 140507 (2009).

[17] Y. Sun and K. Maki, Phys. Rev. B **51**, 6059 (1995).

[18] D. Xu, S. K. Yip, and J. A. Sauls, Phys. Rev. B **51**, 16233 (1995).

[19] V. Mishra, G. Boyd, S. Graser, T. Maier, P. J. Hirschfeld, and D. J. Scalapino, Phys. Rev. B **79**, 094512 (2009).

[20] V. Mishra, S. Graser, and P. J. Hirschfeld, Phys. Rev. B **84**, 014524 (2011).

[21] S. Graser, A. F. Kemper, T. A. Maier, H.-P. Cheng, P. J. Hirschfeld, and D. J. Scalapino, Phys. Rev. B **81**, 214503 (2010).

[22] I. I. Mazin, T. P. Devereaux, J. G. Analytis, Jiun-Haw Chu, I. R. Fisher, B. Muschler, and R. Hackl, Phys. Rev. B **82**, 180502(R) (2010).

[23] K. Suzuki, H. Usui, and K. Kuroki, J. Phys. Soc. Jpn. **80**, 013710 (2011).

[24] M. Yamashita, Y. Senshu, T. Shibauchi, S. Kasahara, K. Hashimoto, D. Watanabe, H. Ikeda, T. Terashima, I. Vekhter, A. B. Vorontsov, and Y. Matsuda, Phys. Rev. B **84**, 060507(R) (2011).

[25] Y. Wang, A. Kreisel, P. J. Hirschfeld, and V. Mishra, Phys. Rev. B **87**, 094504 (2013).

[26] Y. Mizukami, M. Konczykowski, Y. Kawamoto, S. Kurata, S. Kasahara, K. Hashimoto, V. Mishra, A. Kreisel, Y. Wang, P. J. Hirschfeld, Y. Matsuda, and T. Shibauchi, Nat. Commun. **5**, 5657 (2014).

[27] L. Fang, Y. Jia, V. Mishra, C. Chaparro, V. K. Vlasko-Vlasov, A. E. Koshelev, U. Welp, G. W. Crabtree, S. Zhu, N. D. Zhigadlo, S. Katrych, J. Karpinski, and W. K. Kwok, Nat. Commun. **4**, 2655 (2013).

[28] L. Civale, A. D. Marwick, T. K. Worthington, M. A. Kirk, J. R. Thompson, L. Krusin-Elbaum, Y. Sun, J. R. Clem, and F. Holtzberg, Phys. Rev. Lett **67**, 648 (1991).

[29] M. A. Kirk, Cryogenics **33**, 235 (1993).

[30] L. Fang, Y. Jia, J. A. Schlueter, A. Kayani, Z. L. Xiao, H. Claus, U. Welp, A. E. Koshelev, G. W. Crabtree, and W.-K. Kwok, Phys. Rev. B **84**, 140504(R) (2011).

[31] L. Civale, A. D. Marwick, M. W. McElfresh, T. K. Worthington, A. P. Malozemoff, F. H. Holtzberg, J. R. Thompson, and M. A. Kirk, Phys. Rev. Lett. **65**, 1164 (1990).

[32] S. Kasahara, T. Shibauchi, K. Hashimoto, K. Ikada, S. Tonegawa, R. Okazaki, H. Shishido, H. Ikeda, H. Takeya, K. Hirata, T. Terashima, and Y. Matsuda, Phys. Rev. B **81**, 184519 (2010).

[33] M. Nakajima, S. Uchida, K. Kihou, C.-H. Lee, A. Iyo, and H. Eisaki, J. Phys. Soc. Jpn. **81**, 104710 (2012).

[34] SRIM, The Stopping and Range of Ions in Matter, James F. Ziegler, Jochen P. Biersack, and Matthias D. Ziegler.

[35] Y. Nakajima, T. Taen, Y. Tsuchiya, T. Tamegai, H. Kitamura, and T. Murakami, Phys. Rev. B **82**, 220504(R) (2010).

[36] R. Prozorov, M. Konczykowski, M. A. Tanatar, A. Thaler, S. L. Bud'ko, P. C. Canfield, V. Mishra, and P. J. Hirschfeld, Phys. Rev. X **4**, 041032 (2014).

[37] K. Cho, M. Konczykowski, J. Murphy, H. Kim, M. A. Tanatar, W. E. Straszheim, B. Shen, H. H. Wen, and R. Prozorov, Phys. Rev. B **90**, 104514 (2014).

[38] C. J. van der Beek, S. Demirdis, D. Colson, F. Rullier-Albenque, Y. Fasano, T. Shibauchi, Y. Matsuda, S. Kasahara, P. Gierlowski, and M. Konczykowski, J. Phys.: Conf. Ser. **449**, 012023 (2013).

[39] T. Taen, F. Ohtake, H. Akiyama, H. Inoue, Y. Sun, S. Pyon, T. Tamegai, and H. Kitamura, Phys. Rev. B **88**, 224514 (2013).

[40] R. Prozorov and V. G. Kogan, Rep. Prog. Phys. **74**, 124505 (2011).

[41] K. Hashimoto, M. Yamashita, S. Kasahara, Y. Senshu, N. Nakata, S. Tonegawa, K. Ikada, A. Serafin, A. Carrington, T. Terashima, H. Ikeda, T. Shibauchi, and Y. Matsuda, Phys. Rev. B **81**, 220501(R) (2010).

[42] K. Hashimoto, K. Cho, T. Shibauchi, S. Kasahara, Y. Mizukami, R. Katsumata, Y. Tsuruhara, T. Terashima, H. Ikeda, M. A. Tanatar, H. Kitano, N. Salovich, R. W. Giannetta, P. Walmsley, A. Carrington, R. Prozorov, and Y. Matsuda, Science **336**, 1554 (2012).

[43] Y. Nakai, T. Iye, S. Kitagawa, K. Ishida, S. Kasahara, T. Shibauchi, Y. Matsuda, and T. Terashima, Phys. Rev. B **81**, 020503(R) (2010).

[44] J. R. Cooper, Phys. Rev. B **54**, R3753 (1996).

[45] L. Malone, J. D. Fletcher, A. Serafin, A. Carrington, N. D. Zhigadlo, Z. Bukowski, S. Katrych, and J. Karpinski, Phys. Rev. B **79**, 140501 (2009).

[46] Y. Jia, M. Leroux, D. J. Miller, J. G. Wen, W.-K. Kwok, U. Welp, M. W. Rupich, X. Li, S. Sathyamurthy, S. Fleshler, A. P. Malozemoff, A. Kayani, O. Ayala-Valenzuela, and L. Civale, Appl. Phys. Lett. **103**, 122601 (2013).

[47] M. A. Kirk and Y. Yan, Micron **30**, 507 (1999).

[48] See Supplemental Material at http://link.aps.org/supplemental/10.1103/PhysRevB.93.115119 for TRIM calculations showing a mixture of point defects and cascades.

[49] A. C. Durst and P. A. Lee, Phys. Rev. B **65**, 094501 (2002).